# Internal Stresses and Structures Developed During Creep

L. J. CUDDY

Specimens of 304 stainless steel subjected to different thermomechanical histories develop different internal stresses, $\sigma_i$, and different substructures. Creep rate is uniquely related not to the applied stress, $\sigma_A$, but to the effective stress, $\sigma^* = (\sigma_A - \sigma_i)$. Values of $\sigma^*$ are determined from experimental results and $\sigma_i$ calculated from $\sigma_i = (\sigma_A - \sigma^*)$. Results show $\sigma_i$ increases with the applied stress according to $\sigma_i \propto \sigma_A^{1.7}$. Transmission electron microscopic observations show that the density of dislocations within subgrains, $\rho_D$, and the subgrain diameter, $D$, vary with applied stress according to: $\rho_D \propto \sigma_A^K$, $D \propto \sigma_A^{-0.8}$, where $K$ = 1.4 to 2.0. Subgrain misorientation is independent of creep stress, strain, or temperature. The contributions of these structural variables to the internal stress are discussed.

IT has long been recognized that the creep rate of a material cannot be predicted merely by specifying the stress and temperature to which it is subjected. A number of studies have demonstrated the pronounced effect of thermomechanical history, or differences in substructure, upon creep rate.[1-13] Sherby and coworkers[2] made a systematic study of the effects of stress, strain, and temperature histories upon the steady-state creep rate of aluminum. They concluded that variations in history led to substructural changes which affected the creep rate, and that the equation for the steady-state creep rate, $\dot{\epsilon}_S$, could be written:

$$\dot{\epsilon}_S \exp\left(\frac{Q}{RT}\right) = A(S) f(\sigma) \qquad [1]$$

where $A(S)$ is a parameter dependent on structure which is separable from the stress-dependent parameter, $f(\sigma)$. However, Bayce *et al.*[5] subsequently found that no such separation was possible, but that "the effect of stress on creep rate (is) dependent on the substructure," *i.e.*, in Eq. [1] $f(\sigma) \rightarrow f(\sigma, S)$.

An alternate method of incorporating history or structural effects upon creep rate is through use of the concept of an internal, or back, stress.[14-17] As structural changes occur during creep, the effective stress producing deformation is reduced by the development of an internal stress, $\sigma_i$, acting in opposition to the applied stress. Thus, the creep rate is related not to the applied stress, $\sigma_A$, but to the effective stress $\sigma^* = (\sigma_A - \sigma_i)$. Recently, an attempt has been made to determine $\sigma_i$ from results of experiments at elevated temperatures. Nix, Barrett, and coworkers,[18] by means of their "dip test", have determined the critical value of the applied stress which just balances the effective internal stress to reduce the strain-rate to zero. From their analysis they conclude that the maximum of the periodic internal stress is in excess of 90 pct of the applied stress.

In the present study we have developed another method of determining the internal stress which is produced during creep. Toward this end we performed what Sherby and coworkers[2] referred to as "constant-structure" tests. Referring to Fig. 1(*a*), all specimens of a single series of tests are prestrained to the same strain, $\epsilon_p$, at the same stress, $\sigma_p$, and temperature, $T$, to produce as nearly as possible identical structures and identical internal stresses in each. The applied stress is then abruptly reduced to one of the preselected final stresses ($\sigma_1$, $\sigma_2$, $\sigma_3$) and the creep rate immediately after the drop ($\dot{\epsilon}_1$, $\dot{\epsilon}_2$, $\dot{\epsilon}_3$) measured. Assuming that there is no significant change in structure or internal stress during the drop in applied stress, this creep rate is a function of the final applied stress and the internal stress developed during prestraining, *i.e.*

$$\dot{\epsilon} \exp\left(\frac{Q}{RT}\right) = f(\sigma_A - \sigma_i) = f(\sigma^*) \qquad [2]$$

Groups of specimens with different prestraining histories have different $\sigma_i$ and therefore produce different $\dot{\epsilon}$ vs $\sigma_A$ curves, $\alpha$ and $\beta$ in Fig. 1(*b*). From Eq. [2] it is seen that the observed difference in applied stress necessary to maintain a given creep rate in two specimens is a reflection of the difference in their internal stresses. By varying prestraining conditions and observing the corresponding changes in applied stress necessary to maintain a given rate, we have determined the unique value of $\sigma^*$ for that rate. The difference between the observed applied stresses and the effective stress yields the internal stress developed by each set of prestraining conditions, *i.e.*, $\sigma_i = \sigma_A - \sigma^*$.

Along with values of $\sigma_i$ determined in this manner, we examined, by means of transmission electron microscopy, the substructures developed in specimens subjected to a wide variety of creep conditions. Finally, these data were examined for correlations between the variations in the values of $\sigma_i$ and variations in substructure.

## PROCEDURE

Three-in. lengths were cut from $\frac{1}{2}$ in. diam rod of commercial AISI Type 304 stainless steel whose composition is shown in Table I. These were annealed at 1090°C for 30 min to produce a uniform grain size of 74 $\mu$m diam. Threaded-end specimens with a gage section 0.150 in. in diam by 1.438 in. long were machined from the blanks. Specimens were mounted in the constant-stress, tensile apparatus described in a previous publication[19] and soaked for at least 24 hr at the testing temperature to stabilize the structure prior to testing. The load on the specimen, its extension, and

L. J. CUDDY is Senior Scientist, E. C. Bain Laboratory for Fundamental Research, U. S. Steel Corporation, Research Center, Monroeville, Pa.

Manuscript submitted March 14, 1969.

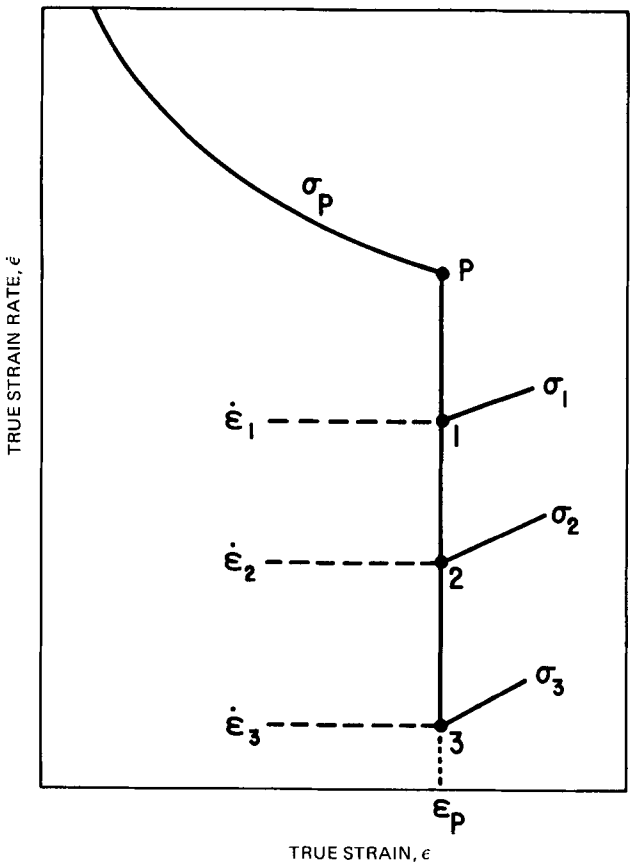


Fig. 1(*a*)—Schematic representation of a series of constant-structure tests.

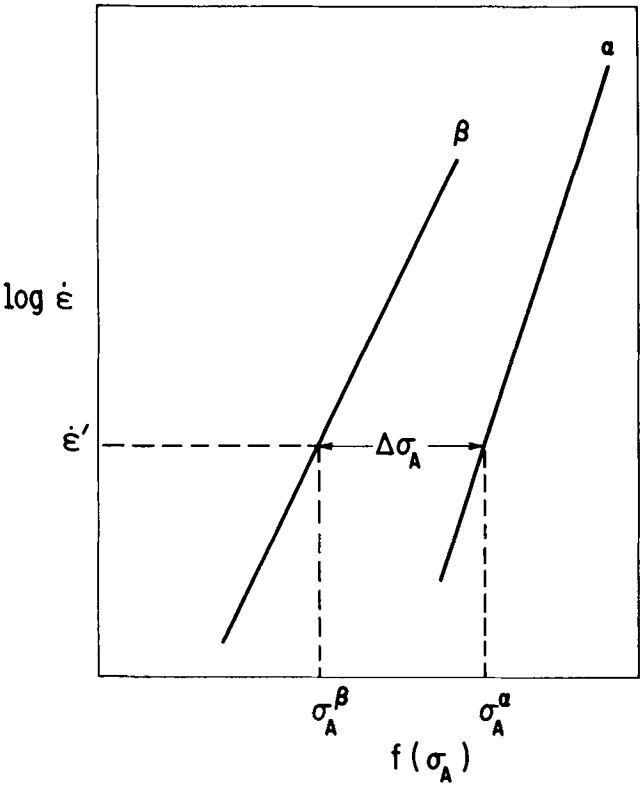


Fig. 1(*b*)—Schematic of creep-rate vs applied stress curves for specimens with different structures and internal stresses.

its temperature were recorded continuously throughout the test. Load, read from a load cell incorporated in series with the specimen, indicated that stress remained constant to within ±0.5 pct. Extension was monitored to within 0.0002 in. by an extensometer fastened to the shoulders of the specimen and equipped with a linear variable differential transformer. Temperatures were read from thermocouples spot-welded to the top and bottom of the gage length and were constant to within ±0.5°C. Stress drops were effected by removing weights from the load pan. Temperature changes of about 15°C required about 10 min and were carried out without removing the load. At the completion of the test the specimen was cooled under load to preserve as well as possible the structure prevailing during the creep test.

Thin films for electron transmission microscopy were prepared from disks cut from the center of the gage section. Six micrographs at 20,000X were taken from each specimen for dislocation density determination. A plastic overlay containing a 30-cm-circumference circle was placed in nine random positions over 3X prints of each micrograph, and the number of dislocations not in cell walls intersecting the circle was counted. Density was computed from

$$\rho_D = \frac{n}{Lt}$$

where $n$ is the number of intersections of dislocations along a length, $L$, of circumference, and $t$ is the film thickness, taken to be 2000Å. Approximately twelve other micrographs at 2000 to 8000X were taken from each specimen. Average subgrain diameters were determined from these by the line intercept method, with the line laid in several directions to minimize orientation effects. Diffraction patterns were taken from the thicker areas of the foils to measure subboundary misorientation by shift of Kikuchi patterns. When an area displaying strong Kikuchi lines was found, patterns were taken in every one of a colony of adjacent subgrains to get the average misorientation. Colonies examined contained from four to ten subgrains. Colonies in at least two different grains were examined in each specimen.

## RESULTS AND DISCUSSION

In preliminary work a series of constant-stress tests and a separate series of temperature-change tests were carried out. Results of the constant-stress tests showed that, except at very low stresses, steady

**Table I. Composition of 304 Stainless Steel**

| Element | Wt Pct |
|---|---|
| C | 0.051 to 0.054 |
| N | 0.043 to 0.046 |
| Cr | 18.5 to 19.7 |
| Ni | 9.5 to 9.8 |
| Mn | 1.61 to 1.62 |
| Si | 0.48 to 0.50 |
| Mo | 0.30 to 0.31 |
| V | 0.028 to 0.029 |
| Ti | <0.02 |
| Cb | <0.02 |
| O | 0.0035 to 0.0041 |

state was not achieved even for true strains as high as 0.25. Eventually a minimum rate is observed at the onset of necking. This minimum rate is higher than the true steady state rate which is observed only in the absence of necking.[20] Rather than attempt to determine the $\dot{\epsilon} - \sigma$ relation from these arbitrary minimum rates, the creep rate at a constant value of strain, 0.15 unless otherwise noted, was used as a basis of comparison for all tests. Measurements at $\epsilon = 0.09$ and 0.24 gave the same $\dot{\epsilon} - \sigma_A$ relations. Using these values it was found that creep rate, $\dot{\epsilon}$, was related to applied stress, $\sigma_A$, through a power law, $\dot{\epsilon} \propto \sigma_A^n$.

Temperature change tests centered at 711°, 809°, and 879°C showed that the apparent activation energy for creep in 304 stainless is:

$$Q = 91 \pm 9 \text{ kcal per mol}$$

This value is independent of both temperature and stress. As a check on this activation energy, the log of the temperature-compensated creep rate $\dot{\epsilon} \exp(91{,}000/RT)$, was plotted against log stress for all the constant stress tests, Fig. 2. The data for temperatures from 704° to 927°C fall on a single curve, indicating that 91,000 cal per mol is the proper value for activation energy for creep of 304 stainless steel.

The relation between creep rate and applied stress illustrated in Fig. 2 reflects not only the direct effect of applied stress upon creep rate, but also includes the effect upon creep rate of differences in structure which yield differences in internal stress developed at the different applied stresses. For example, transmission studies revealed that subgrains were fully formed after 8 to 10 pct of creep strain; once formed,

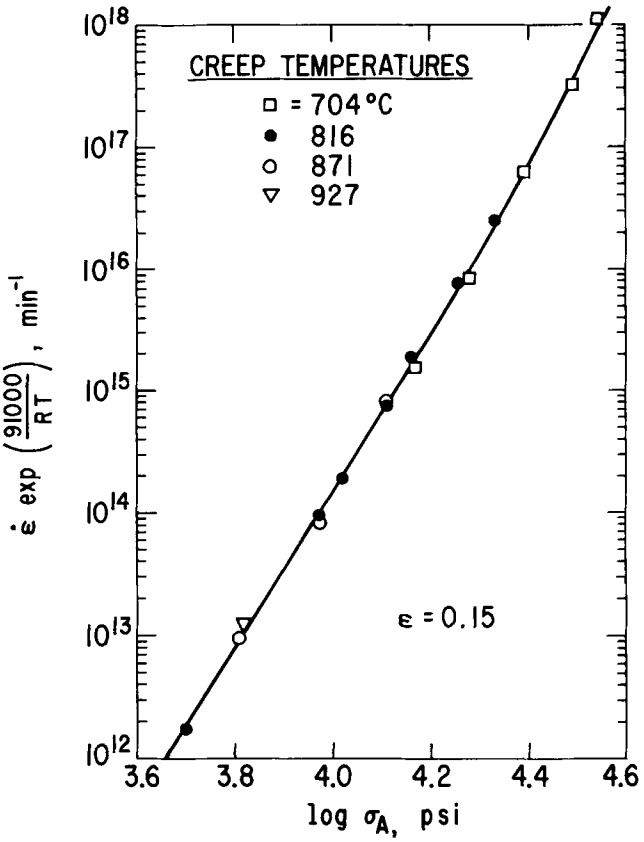


Fig. 2—Dependence of temperature-compensated creep rate on applied stress in constant-stress tests.

their size remained essentially constant. The average subgrain diameter, $D$, decreased markedly with increase in applied stress, $\sigma_A$, Fig. 3. For stresses between 4000 and 35,000 psi the subgrain diameter, $D$, decreased according to

$$D \propto \sigma_A^{-0.8} \quad [3]$$

Fig. 4. These measurements were made on specimens strained from 0.10 to 0.25 at temperatures from 704° to 816°C. No effect of strain or temperature was observed. The density of dislocations not associated with cell walls was measured in foils prepared from specimens elongated at various stresses to strains of approximately 0.23 at temperatures from 704° to 816°C. As shown in Fig. 5, the density increases as

$$\rho_D \propto \sigma_A^K \quad [4]$$

where $K = 1.4$ to 2.0. Between 704° and 816°C, the density is independent of temperature. Such relations between applied stress and substructural variables are apparently quite general since they have been reported for Al,[21-24] Cu,[25] stainless steel,[9,26] Fe-Si,[27,28] and Fe.[8] In many of these observations the temperature independence of the structural variables has been noted.

Subboundary misorientation was determined by the shift in the Kikuchi lines caused by crossing the subboundary. In over 120 observations of specimens strained from 0.07 to 0.29 at stresses from 8000 to 15,500 psi and temperatures from 704° to 816°C, no regular change in misorientation with variation of these parameters was observed. If trends exist, they are obscured by the broad scatter in experimental results. For example, the apparent misorientations in a single cluster of subgrains such as those shown in Fig. 3 may range from 0.08 to 2.5 deg.

Five series of constant-structure tests were performed as outlined above in order to determine values of internal stress. Results of a typical series are shown in Fig. 6. Here all specimens were prestrained approximately 15 pct at 35,800 psi, 704°C after which the applied stress was dropped to one of a series of final stresses indicated at the right of the figure. The temperature-compensated strain rate is plotted against applied stress for the five series of tests in Fig. 7, which also contains the prestraining conditions for each series. The results for all series can be approximated by a power-law relation

$$\dot{\epsilon} \exp\left(\frac{Q}{RT}\right) = A\sigma_A^n$$

where $n$ is dependent upon the prestraining stress. Separate tests showed no dependence of $n$ upon strain, from 0.09 to 0.24, or upon temperature, from 704° to 927°C. It is obvious from Fig. 7 that the creep rate is not a unique function of applied stress. In fact Fig. 8 shows that the curves for different prestrain stresses are similar but displaced from one another by constant values of $\Delta\sigma_A$. According to our discussion above we assume that these differences in applied stress reflect the differences in internal stress developed by the different prestraining stresses, *i.e.*, $\Delta\sigma_i = \Delta\sigma_A$.

Absolute values of $\sigma_i$ developed by each prestraining stress were evaluated by two methods. In the first method, the values of $A$ and $n$ for each curve in Fig. 7 were plotted against the prestrain stress for that

curve, Fig. 9. Extrapolating to $\sigma_P = 0$ gives the values of these parameters for the condition $\sigma_i = 0$, *i.e.*, $\sigma_A = \sigma^*$. This procedure predicts that, at low stresses:

$$\dot{\epsilon} \exp\left(\frac{Q}{RT}\right) = 1.6 \times 10^{-9} \sigma^{*5.8} \text{ min}^{-1}$$

which is shown dotted in Figs. 7 and 8. The $\dot{\epsilon}$ vs $\sigma_A$

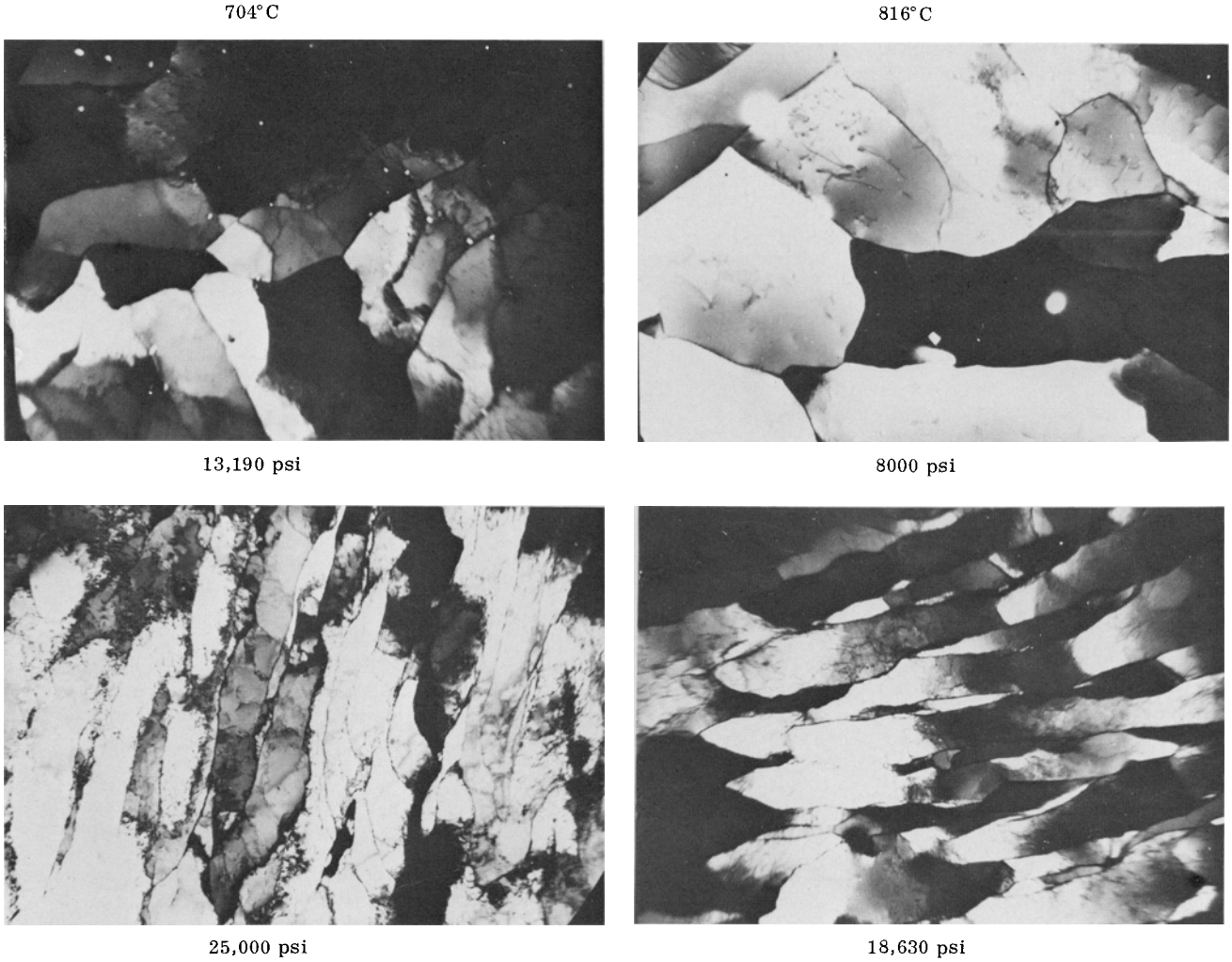


Fig. 3—Subgrains developed in 304 stainless during creep to strains of 0.25. Magnification 4000 times.

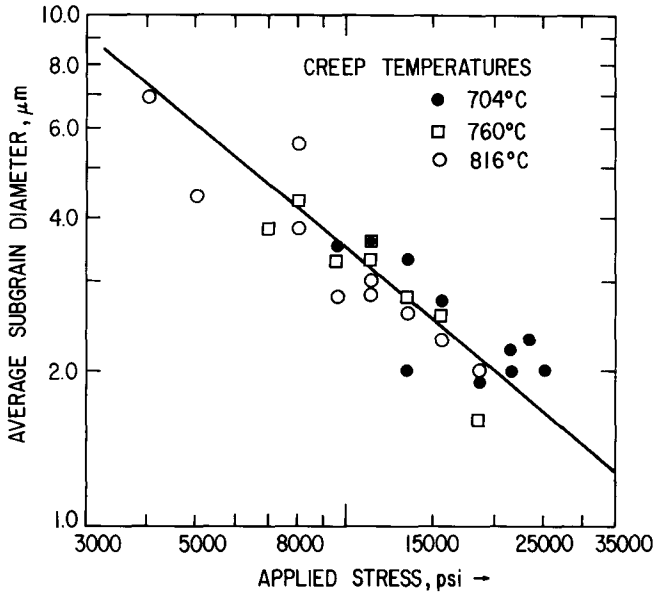


Fig. 4—Average subgrain diameters developed in specimens strained 10 to 25 pct at various creep stresses.

curve for specimens prestrained at 6600 psi lies to the right of this dotted curve by an amount $\Delta\sigma_A = \sigma_i$, the internal stress developed at 6600 psi. Other curves lie farther to the right due to the higher internal stresses developed at higher prestraining stresses. Where they overlap in creep rate we can calculate the difference in internal stress in adjacent curves from $\Delta\sigma_i = \Delta\sigma_A$ at constant $\dot{\epsilon}$. The absolute value of $\sigma_i$ for each $\sigma_P$, obtained from summing up the values of $\Delta\sigma_i$, are shown in Table II.

In the second method, the value of applied stress necessary to maintain a given strain rate after prestraining is plotted against the prestraining stress, Fig. 10. Extrapolating to $\sigma_P = 0$ where $\sigma_i = 0$ and $\sigma_A = \sigma^*$, we obtain the unique value of $\sigma^*$ necessary to maintain each creep rate. These results are shown as the dashed curve in Figs. 7 and 8. Values of $\sigma_i$ are then obtained from $\sigma_i = \sigma_A - \sigma^*$ at constant $\dot{\epsilon}$. These results are also shown in Table II. Results of the two methods are plotted in Fig. 11. The agreement is excellent and indicates that internal stress is related to the prestraining stress by which it was developed according to:

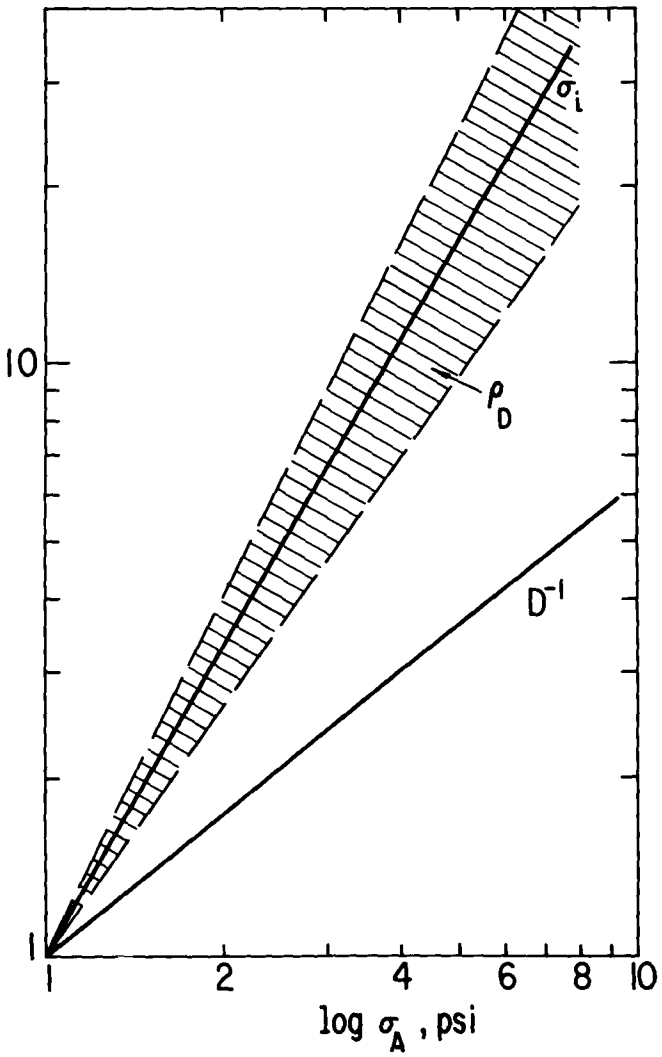


Fig. 12—Increase with applied stress of internal stress, dislocation density, and density of subgrain boundaries.

By studying the variation in the $\dot{\epsilon}$ vs $\sigma_A$ curves for sets of specimens which were prestrained at different stresses, $\sigma_P$, the value of $\sigma^*$ for each $\dot{\epsilon}$ is determined. The internal stress developed by each prestraining stress is calculated from $\sigma_i = \sigma_A - \sigma^*$. Results show $\sigma_i \propto \sigma_P^{1.7}$. Observation by transmission electron microscopy showed that the density of dislocations within subgrains, $\rho_D$, and the subgrain diameter, $D$, varied with applied stress according to:

$$\rho_D \propto \sigma_A^K, \quad D \propto \sigma_A^{-0.8}$$

where $K$ = 1.4 to 2.0. Both were independent of strain and temperature. Subgrain misorientation showed no regular variation with creep stress, strain, or temperature. These results indicate that the internal stress arises from some or all of these structural variables. However, further work is necessary to determine the relative contribution of each.

## ACKNOWLEDGMENTS

The author is grateful to J. C. M. Li, P. J. Wray, O. Richmond, and W. C. Leslie for helpful discussions and for reviewing the manuscript. Special thanks are due to J. C. Raley for competent handling of the experimental work. All are members of this Laboratory.

## REFERENCES

1. A. J. Kennedy: *Proc. Phys. Soc.*, 1949, vol. 62B, p. 501.
2. O. D. Sherby, R. Frenkel, J. Nadeau, and J. E. Dorn: *Trans. TMS-AIME*, 1954, vol. 200, p. 275.
3. T. H. Hazlett and R. D. Hansen: *Trans. ASM*, 1955, vol. 47, p. 508.
4. O. D. Sherby, T. A. Trozera, and J. E. Dorn: *Trans. ASTM*, 1956, vol. 56, p. 789.
5. A. E. Bayce, W. D. Ludemann, L. A. Shepard, and J. E. Dorn: *Trans. ASM*, 1960, vol. 52, p. 451.
6. F. Garofalo, F. von Gemmingen, and W. F. Domis: *Trans. ASM*, 1961, vol. 54, p. 430.
7. W. M. Yim and N. J. Grant: *Trans. TMS-AIME*, 1963, vol. 227, p. 868.
8. A. Goldberg: *J. Iron Steel Inst.*, 1966, vol. 204, p. 268.
9. J. A. Mazza and G. Willoughby: *J. Iron Steel Inst.*, 1966, vol. 204, p. 718.
10. S. K. Mitra and D. McLean: *Metals Sci. J.*, 1967, vol. 1, p. 192.
11. L. K. Gordienko and P. V. Zubarev: *Metalloved. i Term. Obrabotka Metal.*, 1967, no. 6, p. 12.
12. Y. Ishida: *Trans. Japan Inst. Metals*, 1968, vol. 9, p. 120.
13. G. R. Wilms: *J. Inst. Met.*, 1954-55, vol 83, p. 427.
14. A. S. Nowick and E. S. Machlin: *J. Appl. Phys.*, 1947, vol. 18, p. 79.
15. F. Garofalo: *Fundamentals of Creep and Creep Rupture in Metals*, p. 123, The Macmillan Co., New York, 1965.
16. J. E. Dorn: *Energetics in Metallurgical Phenomena*, vol. 1, p. 241, Gordon and Breach, New York, 1965.
17. J. J. Jonas: *Acta Met.*, 1969, vol. 17, p. 397.
18. W. D. Nix and C. R. Barrett: presented at the ASM Symposium, Dislocation Climb and High-Temperature Creep Processes, Detroit, October, 1968.
19. F. Garofalo, O. Richmond, and W. F. Domis: *J. Basic Eng.*, 1962, p. 287.
20. P. J. Wray and O. Richmond: *J. Appl. Phys.*, 1968, vol. 39, p. 5754.
21. N. J. Grant and A. R. Chaudhuri: *Creep and Recovery*, p. 284, Am. Soc. Metals, 1957.
22. D. McLean: *J. Inst. Met.*, 1951-52, vol. 80, p. 507.
23. F. H. Hammad and W. D. Nix: *Trans. ASM*, 1966, vol. 59, p. 94.
24. H. J. McQueen, W. A. Wong, and J. J. Jonas: *Can. J. Phys.*, 1967, vol. 45, p. 1225.
25. V. P. Gupta and P. R. Strutt: *Can. J. Phys.*, 1967, vol. 45, p. 1213.
26. F. Garofalo, O. Richmond, W. F. Domis, and F. von Gemmingen: *Joint International Conference on Creep*, p. 1, The Institution of Mech. Eng., London, 1963.
27. J. L. Lytton, C. R. Barrett, and O. D. Sherby: *Trans. TMS-AIME*, 1965, vol. 233, p. 1399.
28. C. R. Barrett and W. D. Nix: *Acta Met.*, 1965, vol. 13, p. 1247.